LIMNOLOGY and OCEANOGRAPHY

ASLO

Limnol. Oceanogr. 9999, 2023, 1–20

doi: 10.1002/lno.12408

Drivers behind the diversity and distribution of a widespread midwater narcomedusa

Gerlien Verhaegen [1,2*] **Mehul Naresh Sangekar** [2] **Bastian Bentlage** [3] **Henk-Jan Hoving** [4] **Allen G. Collins** [5] **Dhugal Lindsay** [2]

[1]HYIG ARJEL, Functional Ecology, Alfred Wegener Institute Helmholtz Centre for Polar and Marine Research (AWI), Bremerhaven, Germany
[2]Institute for Extra-cutting-edge Science and Technology Avant-garde Research (X-STAR), Japan Agency for Marine-Earth Science and Technology (JAMSTEC), Yokosuka, Japan
[3]Marine Laboratory, University of Guam, Mangilao, Guam, USA
[4]Marine Ecology, GEOMAR Helmholtz Centre for Ocean Research Kiel, Kiel, Germany
[5]National Systematics Laboratory of NOAA's Fisheries Service, National Museum of Natural History, Smithsonian Institution, Washington, USA

Abstract

Narcomedusae play a key role as top-down regulators in the midwater, the largest and most understudied biome on Earth. Here, we used ecological niche modeling in three-dimensions (3D), ecomorphology, and phylogeny, to answer evolutionary and ecological questions about the widespread narcomedusan genus *Solmissus*. Our phylogenetic analyses confirmed that *Solmissus incisa* represents a complex of several cryptic species. Both the different genetic clades and tentacle morphotypes were widespread and often overlapped geographically-the main difference in their distribution and ecological niche being depth. This demonstrated the importance of including the third dimension when modeling the distribution of pelagic species. Contrary to our hypothesis, we found the modeled distribution of the *Solmissus* genus ($n = 1444$) and both tentacle morphotypes to be mostly driven by low dissolved oxygen values and a salinity of 34, and slightly by depth and temperature. *Solmissus* spp. were reproducing all year round, with specimens reproducing in slightly warmer waters (up to 1.25°C warmer). Our results suggest that *Solmissus* spp. will likely come out as climate change winners by expanding their distribution when facing ocean deoxygenation and by increasing their reproduction due to global warming. However, because most available midwater data comes from the northern Pacific, this sampling bias was undoubtedly reflected in the output of our ecological niche models, which should be assessed carefully. Our study illustrated the value of online databases including imagery and videography records, for studying midwater organisms and treating midwater biogeographic regions as 3D spaces.

*Correspondence: gerlienverhaegen@hotmail.com

Additional Supporting Information may be found in the online version of this article.

Author Contribution Statement: Study concept: D.L., G.V., and B.B. Presence data collection: G.V., D.L., and H.-J.H. Environmental data formatting and coding: M.N.S. Morphological analysis of presence data: G.V. DNA extraction and amplification: A.G.C. Phylogenetic analyses: B.B. Ecological niche modeling: G.V. Statistics and graphs: G.V. Figures: G.V. and B.B. Writing: G.V., B.B., and A.G.C. Proofread and approved the final submitted manuscript: all.

The ocean's midwater (between the euphotic zone and seafloor) is the largest continuous biome on our planet (Robison 2004), is drastically under-sampled (Webb et al. 2010), and many of the species that inhabit it are likely yet to be discovered (Robison 2004). At the same time, pelagic ecosystems are widely acknowledged for their relevance in ecosystem services (Thurber et al. 2014; St. John et al. 2016). For instance, the dark midwater realm is a heterotrophic system where energy input comes from sinking marine snow particles and where carbon is stored and reprocessed by a multitude of organisms. Many of the organisms that inhabit the mesopelagic and upper bathypelagic zones migrate to feed overnight in shallower waters, respiring and defecating during the day at depth. By vertically transporting organic material from the surface, the midwater plays a major role in carbon sequestration (Brierley 2014), and thus in climate regulation. Midwater

organisms serve as food for marine mammals and large pelagic fishes and are thus relevant to fisheries and ecotourism (Thurber et al. 2014; St. John et al. 2016). Our knowledge gap in midwater communities is a problem because it hampers our ability to predict how global change and anthropogenic pressures will affect this essential and vast ecosystem (Webb et al. 2010; Drazen et al. 2020). One approach to investigate these hard-to-sample midwater organisms is the integration of in situ observations and ecological niche modeling.

Sillero (2011) proposed the term ecological niche modeling to encompass models that infer the distribution of suitable habitats of species. Correlative ecological niche models, as opposed to mechanistic ones, are advantageous because they use distribution data of species to statistically infer associations of species distributions with environmental data in a geographic information system to infer the species potential or realized niche (sensu Hutchinson 1957, *see* Sillero 2011), depending on the type of correlative model and occurrence data used (Jiménez-Valverde et al. 2008). These models have largely been applied to terrestrial systems and their use in the marine realm remains relatively scarce (Robinson et al. 2011). Because most implementations treat environments as flat two-dimensional (2D) spaces, their use is appropriate when investigating terrestrial systems, or when studying marine species restricted to shallow waters or the seabed (Bentlage et al. 2013). Using ecological niche models to study 3D systems such as the midwater is more challenging (Bentlage et al. 2013; Duffy and Chown 2017). Marine studies have often paired environmental variables from the sea surface to species occurrence records from deeper waters, even though environmental conditions differ between the surface and deeper water layers, sometimes leading to misrepresentations and misleading results (Duffy and Chown 2017). Accounting for the third dimension is also important for midwater conservation policies (Venegas-Li et al. 2017; Levin et al. 2018). To address these issues, explicit 3D modeling approaches are being developed (Bentlage et al. 2013; Duffy and Chown 2017; Pérez-Costas et al. 2019), only a handful of which have been applied to midwater taxa, including lanternfish (Freer et al. 2020), and gelatinous zooplankton (Bentlage et al. 2013; Pantiukhin et al. 2023). In this study, we use 3D ecological niche modeling to investigate the ecology and distribution of a genus of widespread midwater jellyfish in the hydrozoan order Narcomedusae (Cnidaria: Hydrozoa).

Gelatinous zooplankton dominate the midwater trophic web, playing important roles, for example, as filter feeders and predators (e.g., Robison 2004; Choy et al. 2017). Among the active hunters, narcomedusae are specialized to feed on other gelatinous animals (but *see* below). By top-down regulation of other gelatinous predators, narcomedusae play a key role in maintaining a well-balanced midwater ecosystem (e.g., Robison 2004; Choy et al. 2017). The genus of dinner plate jellyfishes or *Solmissus* Haeckel, 1879 is one of the most common and widespread midwater narcomedusae. These bioluminescent jellyfish (Haddock and Case 1999) ingest a large diversity of gelatinous zooplankton, as well as pteropod molluscs, krill, annelids, and fishes—some of which may have been bycatch from the stomachs of ingested prey (Larson et al. 1989; Raskoff 2002; Choy et al. 2017; Hidaka-Umetsu and Lindsay 2018). They also host developing larval narcomedusae (Osborn 2000) and hyperiid amphipod parasitoids (Gasca et al. 2007, 2015). In at least one cryptic "*Solmissus incisa*" species, spherical oocytes develop into opaque spheres and then "parasitic" planula larvae arise on the external walls of the stomach pouches (Lucas and Reed 2009). Despite being widespread and familiar, the taxonomy and phylogeny of *Solmissus* remain largely unresolved. *Solmissus* currently has three widely accepted species [*S. albescens* (Gegenbaur, 1857), *S. marshalli* Agassiz & Mayer, 1902, and *S. incisa* (Fewkes, 1886)], two uncertain species [*S. bleekii* Haeckel, 1879, and *S. faberi* Haeckel, 1879], and a potentially invalid species *S. atlantica* Zamponi, 1983 (Genzano et al. 2008). *Solmissus incisa* has been suggested to represent a complex of several cryptic species (Toyokawa et al. 1998; Lindsay et al. 2015), illustrating that even for the accepted species, confusion exists.

In this study, we used 3D ecological niche modeling, ecomorphology, and phylogeny, to answer evolutionary and ecological questions about *Solmissus* spp. Our first objective was to provide valuable information on the differentiation and speciation processes of holoplanktonic species within the midwater. For this, we tested the hypothesis that the genus *Solmissus* is indeed more diverse than currently known, with *S. incisa* representing a cryptic species complex. We then explored potential drivers behind this hidden diversity. We hypothesized that differences in geographic and environmental niches drive differentiation. We also tested whether a desynchronization of reproduction among "*S. incisa*" morphotypes could be another differentiation factor. Our second objective was to provide insights into how environmental change will affect the distribution and reproduction of this top-down regulator of the midwater gelatinous fauna. Here, we hypothesized that temperature and depth, and to a lesser extent salinity and dissolved oxygen, would be the main environmental factors affecting both reproduction and the global distribution of *Solmissus* spp. This was previously found for other hydromedusae, although studies targeting midwater species had very restricted geographical study areas (Raskoff 2001; Kawamura and Kubota 2008; Hoving et al. 2020; Mańko et al. 2020; Pantiukhin et al. 2023).

Methods

Presence data

Two main occurrence datasets were used for *Solmissus* spp. One containing records for the genus *Solmissus* retrieved from the Ocean Biodiversity Information System (OBIS; https://obis.org/) which included usable depths (i.e., with exact depth

values or depth ranges that were less than 400 m), and a second dataset specifically built for this study and which only comprised presence data ($n = 1444$) that included either a photo, video, or a morphological description of the observed specimen(s). This was done for two reasons: first, to check the quality of our data and ensure a proper identification to genus level for all our observations (Lindsay et al. 2017), and second, to obtain morphological data (e.g., tentacle number, reproductive stage) for our subsequent analyses. Our occurrence data came from three types of sources: online (deep sea) databases ($n = 970$, 67.2%), unpublished data (i.e., unpublished records or records for which the morphological data were unpublished) ($n = 434$, 30.0%), and from the literature ($n = 40$, 2.8%) (Table 1). The minimum required metadata was observation date, latitude, longitude, and depth. For depth, we either took the actual depth of the observation (e.g., from in situ photography), or the average depth between minimum and maximum depths in the case of video footage [e.g., remotely operated vehicle (ROV) footage following the jellyfish], or a net cast. For net samples, we only included records from nets that did not sample through too many depth layers (e.g., Multi Plankton Sampler or "multinets"). Additional metadata such as salinity, temperature, or dissolved oxygen coming from in situ measurements were included in the database when available. The complete dataset can be found in Supporting Information Table S1.

Tentacle number and (a)biotic factors

Tentacle number is one of the many diagnostic characteristics for Hydromedusae species (Bouillon et al. 2006). While this character alone is not enough for species delimitation, it is one that can be clearly discerned from in situ optical data and does not require the sampling of individuals, at least in Narcomedusae with few, thick, primary tentacles. Therefore, in addition to the *Solmissus* spp. records that included information on tentacle number in their description, tentacle number was counted for "*S. incisa*" specimens for which a photograph or a video was available. As it is not uncommon for specimens to be missing some tentacles, we estimated the "real" tentacle number by assuming there was one tentacle per stomach pouch. Histograms were made to assess whether the distribution of tentacle number was uni-, bi-, tri-, or multimodal. Based on these histograms, records labeled as "*S. incisa*" were divided into two tentacle morphotypes for subsequent analyses: "less than 28 tentacles" (hereafter "< 28T") and "more than or equal to 28 tentacles" ("≥ 28T") (*see* Results section). These two tentacle morphotypes were also applied to additional occurrences for which an exact tentacle count was impossible (e.g., blurry footage, part of the disk not photographed, etc.) but a rough estimate was still possible (e.g., when a minimum of 28 tentacles could be counted). We then tested if the number of tentacles could be predicted by in situ environmental variables (salinity, temperature, depth, and dissolved oxygen) by running generalized linear models. The diagnostics are given in Supporting Information Figs. S1–S4.

Three biotic factors were assessed from the observed specimens: "signs of predation" (e.g., tentacles or part of disk missing), "presence of prey in the stomach," and "presence of ectoparasite." We tested if these biotic factors could be influenced by depth, tentacle number, or the interaction of depth with tentacle number by running three separate binomial generalized linear models. The following hypotheses were tested: (1) *Solmissus* specimens with higher tentacle numbers could be found at depths with higher predator attack rates, to minimize the effects of tentacle loss through predation; (2) higher tentacle numbers could be a way to increase hunting success at depths with fewer prey; and (3) specimens with fewer tentacles could have fewer ectoparasites due to lower encounter rates. All generalized linear models in this study were run in R v. 4.0.3 (R Core Team 2023) using the *lme4* package (Bates et al. 2015) and by stepwise dropping of non-significant factors based on Type II Wald χ^2 tests of the *Anova* function from the *car* package (Fox and Weisberg 2011).

Phylogeny and morphotypes

DNA was extracted from 18 *Solmissus* specimens sampled off Japan, California, and Eastern Antarctica (Supporting Information Table S2). Extraction of DNA was carried out using an AutoGenPrep 965 liquid handling robot (AutoGen) in accordance with the manufacturer's instructions for whole blood extractions. Mitochondrial 16S and COI were amplified using previously published primers (16S: Cunningham and Buss 1993; COI: Folmer et al. 1994). PCR thermocycling was conducted in 10 μL reactions containing 1X reaction buffer, 1X BSA, 0.08 mmol L^{-1} of dNTPs, 0.032 mmol L^{-1} of MgCl, 0.24 μmol L^{-1} of each primer, 1 unit of Taq and 1 μL of genomic DNA extract with initial denaturation at 95°C for 4 min, followed by 35 cycles of 95°C denaturation for 30 s, 48°C annealing for 30 s, 72°C extension for 60 s, with final 72°C extension for 5 min. Amplicons were sequenced in both directions via Sanger sequencing, using BigDye Terminator v. 3.1 Kit (Applied Biosystems) and the same primers used for PCR amplification. Forward and reverse reads were assembled into contigs using GENEIOUS v. R10-Prime 2021 (Biomatters).

Newly generated sequences ($n = 18$ for 16S and $n = 6$ for COI) and publicly available sequence data ($n = 6$ for 16S and $n = 4$ for COI) (Supporting Information Table S2) were aligned using MAFFT v. 7.453 (Katoh and Standley 2013) with default run parameters. As outgroups, we used *Cunina octonaria* (sample ID DLSI188) and *Pegantha martagon* (DLSI040) for 16S, and *Aegina citrea* (JAMSTEC_211747 and JAMSTEC_151552) for COI, for their phylogenetic proximity with the genus *Solmissus* (Lindsay et al. 2017; Bentlage et al. 2018). Ambiguous alignment positions were removed using Gblocks v. 0.91b (Castresana 2000), allowing for smaller final blocks, gap positions within final blocks, and less strict flanking positions.

Table 1. The data source for the occurrence dataset of *Solmissus* spp. compiled during this study. All records came with some morphological information (e.g., description, photography, or videography). The pruned datasets were obtained by keeping only one observation per 1° latitude/longitude per closest corresponding depth layer (*see* below) in the Northern Pacific, but by keeping all other observations from other regions. Abbreviations: ENMs = ecological niche models, GEOMAR = Helmholtz Centre for Ocean Research Kiel, HOV = human-occupied vehicle, JAMSTEC = Japan Agency for Marine-Earth Science and Technology, MBARI = Monterey Bay Aquarium Research Institute, NOAA = National Oceanic and Atmospheric Administration, ONC = Ocean Networks Canada, PELAGIOS = Pelagic In situ Observation System, and ROV = remotely operated vehicle.

Source type	Source	Affiliation	Link and/or reference	Records (*n*)	Pruned out records used in the ENMs (*n*)
Online database	FathomNet	MBARI	http://fathomnet.org/fathomnet/#/ (Katija et al. 2022)	411	116
	SeaTube pro	ONC	https://data.oceannetworks.ca/SeaTube	251	149
	JAMSTEC E-library of deep-sea images (J-EDI)	JAMSTEC	https://www.godac.jamstec.go.jp/jedi/e/index.html	221	102
	MBARI Deep-Sea guide	MBARI	http://dsg.mbari.org/dsg/home (Jacobsen Stout et al. 2019)	62	18
	YouTube	Schmidt Ocean Institute	https://www.youtube.com/c/SchmidtOcean	25	25
Unpublished data	ROV *HYPER-DOLPHIN*	JAMSTEC	/	296	90
	ROV *global explorer*	University of Alaska Fairbanks	/	90	46
	ROV *deep discoverer*	NOAA/University of Hawaii	/	15	13
	PELAGIOS (Hoving et al. 2019)	GEOMAR	/	15	15
	HOV *JAGO*	GEOMAR	/	7	7
	Net sampling during CEAMARC	JAMSTEC	/	5	5
	HOV *SHINKAI 2000*	JAMSTEC	/	4	3
	ROV observation	Subsea 7	/	1	1
	Tucker trawl specimen	MBARI	http://n2t.net/ark:/65665/3cd2bd54d-c056-4a5f-8638-331c69a2dc39	1	1
Literature	(Hartman and Emery 1956; Peres 1959; Larson et al. 1989; Mills et al. 1996; Toyokawa et al. 1998; Osborn 2000; Vinogradov and Vereshchaka 2006; Lucas and Reed 2009; Ortman et al. 2010)			40	33
Total				1444	624

Models of sequence evolution for both 16S and COI were inferred using jModelTest v. 2.1.10 (Darriba et al. 2012) using three substitution schemes, including estimation of invariant sites (+I) and rate heterogeneity (+G); the best fitting model was identified using corrected AIC scores. Maximum likelihood phylogenies, including 1000 non-parametric bootstrap trees were inferred using RAxML v. 8.2.12 (Stamatakis 2014). Bayesian posterior probabilities were estimates using two separate runs with four chains each in MrBayes v. 3.2.6 (Huelsenbeck and Ronquist 2001). The MCMC sampler was run for 10,000,000 generations with trees being sampled every 1000 generations. The first 25% of the MCMC chains were discarded as burn-in.

Vertical migration

Based on their location, date, and time, we split all our *Solmissus* spp. occurrences into daytime (i.e., the period between sunrise and sunset) and nighttime observations using the NOAA Solar Calculator (https://gml.noaa.gov/grad/solcalc/). The presence of a vertical migration was then tested by comparing the median depths between the daytime and nighttime observations through a Mann–Whitney test.

The presence of a vertical migration was then tested for the < 28T and ≥ 28T morphotypes, separately.

Ecological niche modeling in 3D

Ecological niche models in 3D were conducted for the genus *Solmissus*, and the "*S. incisa*" < 28T and ≥ 28T morphotypes. Models at the genus level were either conducted with the OBIS dataset, with occurrences that included usable depth (Fig. 1A), or with all *Solmissus* occurrences from our compiled dataset, which included records for *S. albescens*, *S. marshalli*, *S.* "nematocyst" morphotype (*see* below), and all "*S. incisa*" (Fig. 1B). Due to the lack of reliable absence data available for midwater species, two presence-only models were conducted every time for comparison, namely Maxent (Phillips et al. 2006) and the niche of occurrence (NOO) (García-Roselló et al. 2019). Maxent is a general-purpose machine learning algorithm based on the principle of maximum entropy that contrasts the conditions between known presence locations and the whole study area (represented by background points) to estimate relative occurrences rates, which can be transformed into the probability of presence (Phillips et al. 2006). By contrast, NOO is a more simplistic model where only the environmental space of the presence locations is considered, and the probability of presence is inferred from computing Kernel density estimations. Both Maxent and NOO can be applied with a 3D approach. For Maxent, Bentlage et al. (2013) proposed a straightforward method by using oceanographic environmental data grids available for different depth layers within the water column and combining them into a large 2D grid by transforming their latitudes based on their associated depth. In other words, a long strip of equirectangular grids is created in which each adjacent grid corresponds to consecutive depth layers. For NOO3D models, however, the same depth-associated oceanographic grids and the presence data (latitude, longitude, depth) are used to define a true 3D geographical extent (i.e., the most probable accessible area for the targeted species) on which the analyses are based (Pérez-Costas et al. 2019).

Both NOO3D and Maxent are affected by a non-random sampling of presence observations within the environmental space. As most of our observations came from the Northern Pacific, primarily from areas near the Japan Agency for Marine-Earth Science and Technology off Japan, near the Ocean Networks Canada installation off Canada, and near the Monterey Bay Aquarium Research Institute in and around Monterey Bay, we pruned out our presence data for this region to only keep one observation per 1° latitude/longitude per closest corresponding depth layer (*see* below), therefore reducing our used total observations from 1444 to 624 (Table 1). As environmental variables for our 3D models, we used the annual objectively analyzed mean temperature (°C) (Locarnini et al. 2018), salinity (Zweng et al. 2018), and dissolved oxygen (μmol kg^{-1}) (Garcia et al. 2018) grids available from World Ocean Atlas 2018 (https://www.ncei.noaa.gov/access/world-ocean-atlas-2018/). We selected the average decades year as the available decadal period (between 1955 and 2017 for temperature and salinity, 1960–2017 for dissolved oxygen), 1° latitude–longitude as grid resolution, and 64 "whole world" depth layers, located between 50 and 2700 m, as extent. These depth layers were spaced out every 5 m in the upper 100 m, 25 m for the 100–500 m depths, 50 m for the 500–2000 m, and 100 m for the remaining depths until 2700 m. We created a Python code to convert the World Ocean Atlas 2018 grids to depth-layered ASCII grids compatible with Maxent and ModestR, and to create additional grids to include depth as a variable as well (https://github.com/jam-imaging/WOA2018-convertor). The multicollinearity of the environmental variables within the 3D geographic extent was checked through a variance inflation factor (VIF) analysis (Dormann et al. 2013) with ModestR v.6.5 (https://www.modestr.es/sweb/index.php). As no multicollinearity was found, with all VIF < 10, we kept all four environmental variables in our ecological niche models (VIFs: temperature = 1.94, salinity = 1.30, dissolved oxygen = 1.20, and depth = 1.68).

For our Maxent models (using Maxent v.3.4.4), different simulations were first conducted to select the optimal number of background points and whether to use the full extent or target-group backgrounds (Barber et al. 2020), in an effort to correct for sampling bias. The target-group backgrounds were created by selecting the marine environment within a radius of 35 km of the presence points in each depth layer. The distribution of each of the environmental variables was compared for 10,000, 20,000, and 50,000 randomly selected points within these target-group backgrounds, or for 10,000, 20,000, 50,000, and 200,000 random background points for the full extent (Supporting Information Figs. S5–S9). As little difference in distribution was observed, we opted to use 10,000 points for the target-group background models, and 50,000 points for the full-extent models, as a compromise between precision and computational time. The optimal model parameters, namely the adequate combination of feature classes [linear (L), quadratic (Q), product (P), threshold (T), and hinge (H)], and the regularization multiplier (1, 1.5, 2, 2.5, 3, 3.5, or 4) were selected based on the models with the lowest AICc value, using the R package *ENMeval* v. 2.0.4. (Kass et al. 2021) with its spatial cross-validation function "checkerboard2". The final Maxent models were performed with 10 replicated runs per model (i.e., the final model was the average of the multiple runs) using the following additional settings: output = cloglog, random test percentage = 0%, replicated run type = crossvalidate, maximum iterations = 500, convergence threshold = 0.00001, adjust sample radius = 0, default prevalence = 0.5, and apply threshold rule = minimum training presence. We also obtained the relative contribution and the response curves for the four environmental variables. As model performance metrics, we provided the training and test area under the curve (AUC), as well as the continuous Boyce index (CBI) (Boyce et al. 2002). Unlike the AUC metrics

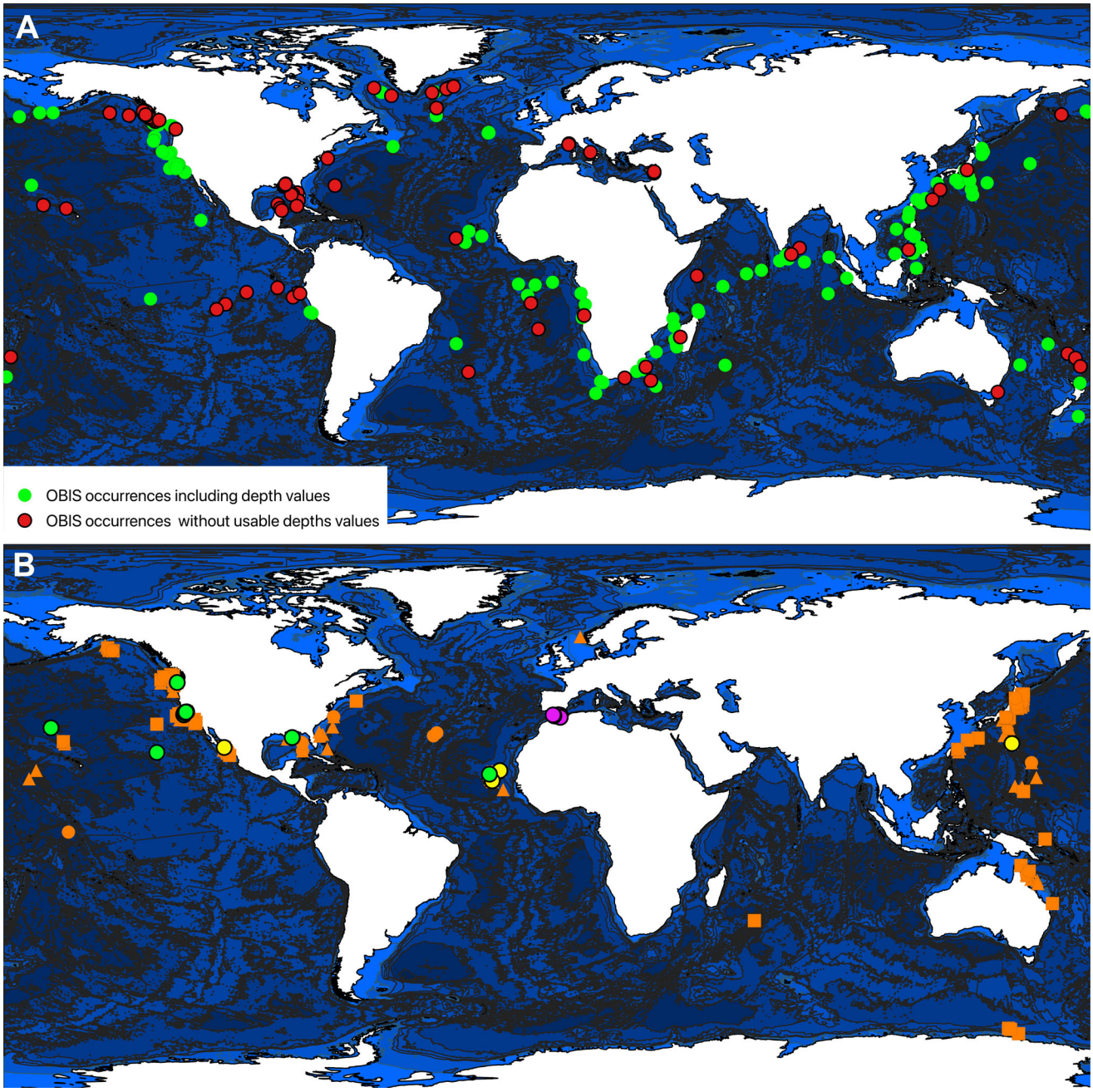

Fig. 1. Occurrences of *Solmissus*. (**A**) Occurrence records available from OBIS for the genus *Solmissus*. Green = occurrences with depth values, red = occurrences without or unprecise depth values. (**B**) Occurrences of the genus *Solmissus* associated with morphological data that was compiled in this study. Purple = *S. albescens*, yellow = *S. marshalli*, orange = "*S. incisa*" (triangle = the "less than 28 tentacles" morphotype, square = the "more than or equal to 28 tentacles" morphotype, circle = with an unknown number of tentacles), and green = the "nematocyst" morphotype.

(historically widely used due to lack of alternatives), the CBI [with values ranging between −1 (poorest fit) and +1 (perfect fit), with negative values indicating the performance of the model is not better than random], is a robust measurement for presence-background and presence-only models. As models ran with background points from the full extent scored better than the ones with target-group background points (Supporting Information Table S3), we only present the results of the former.

We ran our NOO3D models in ModestR following the available tutorials (https://www.modestr.es/sweb/Manual_Tutorial.html), assigning present points to the nearest depth layers, and by using all 64 depth layers. The following Kernel options were selected: smoothing = 1, visual filtering = by

habitat, range = full layer, threshold mode = minimal density at presence. Due to a lack of false positive rate information with NOO models, as a model performance metric we calculated instead pseudo-AUC using a fraction of the total study predicted present as proposed by Phillips (2017). We did not run a NOO3D with the OBIS dataset as its Maxent model scored a mediocre CBI.

Reproduction

A series of analyses were conducted to characterize the reproduction of the whole *Solmissus* genus and the two < 28T and ≥ 28T morphotypes. First, we used χ^2 tests to examine whether season (with winter = January–March, and the other seasons the sequentially following 3-month periods) had a significant effect on the presence of visible oocytes or opaque spheres, a proxy for reproduction, for individuals within the Northern Hemisphere. In a series of Mann–Whitney tests, we then tested if reproductive state was influenced by tentacle number, and the in situ measured variables depth, temperature, salinity, and dissolved oxygen. These statistics were run with PAST v. 4.04 (Hammer et al. 2001).

Results

Presence data

A total of 2914 occurrence records for the genus *Solmissus* were available on OBIS, 2704 (92.8%) of which included usable depth information (data accessed on 04 July 2022) (Fig. 1A). Most of these records (87.4% of occurrences) were part of the Video Annotation and Reference System (Schlining and Jacobsen 2006) database, with all records located along the Western United States coastline. The remaining records were spread worldwide, except for the Arctic and Southern oceans. While nearly all these *Solmissus* spp. records (> 98.2%) came with minimum and maximum depth values, none included media (e.g., photography or videography) or a morphological description of the recorded specimen, with only 15.0% of the records identified to species level.

A total of 1444 presence data (latitude, longitude, and depth) for the genus *Solmissus* associated with some morphological information (e.g., image, video, or description) was newly compiled together for this study (Fig. 1B; Supporting Information Table S1). All subsequent analyses and results were made using this dataset. The data was collected for the period 1951–2022, with nearly all occurrences located in the Northern Hemisphere (97.6%), within the Pacific Ocean (95.0%), and collected during daylight (88.1%). Data from other oceans (Atlantic Ocean 4.5%, Southern Ocean 0.3%, and Indian Ocean 0.1%) or collected during nighttime (8.8%, data with unknown dive time 3.1%) remained scarce. No occurrences were found for the Arctic Ocean.

Tentacle number and (a)biotic factors

Tentacles were counted for a total of 814 "*S. incisa*" individuals, with tentacle numbers varying between 12 and 41, with a median of 26 tentacles. Tentacle number followed a trimodal distribution (Fig. 2B), with a division at around 27 tentacles, with two main peaks based on the Kernel Density Estimation (i.e., a smooth estimator of the histogram) at 23 and 29 tentacles, and a smaller peak at 18–19 tentacles The highest frequency of individuals had either 24 tentacles (8.7% of all individuals) or 30 tentacles (9.7%).

In situ conductivity, temperature, and depth (CTD) data and measurements of dissolved oxygen were available for 539 *Solmissus* observations for which we could count the number of tentacles. As strong multicollinearity was found among all four explanatory variables (depth, temperature, salinity, and dissolved oxygen) (Supporting Information Fig. S10), we tested their effects on tentacle number in four separate generalized linear models. We found a positive effect of depth, and negative effects for temperature and dissolved oxygen, but no effect of salinity on tentacle number (Supporting Information Fig. S11; Supporting Information Table S4).

No link was found between tentacle number, and the interaction of depth and tentacle number, with the biotic factors "signs of predation," "presence of prey in the stomach," or "presence of ectoparasites." Our hypotheses that tentacle number was somehow an adaption to these biotic factors were therefore rejected. We did however find an effect of depth, with higher "signs of predation" but fewer "presence of prey in stomach" in deeper waters, but no effect of depth on the presence of ectoparasites (Fig. 3; Supporting Information Table S5).

Phylogeny and morphotypes

Both mitochondrial 16S and COI showed that *S. incisa* individuals with more than 28 tentacles formed a monophyletic group with high bootstrap support and posterior probability (clade D; Fig. 2; Supporting Information Fig. S12). We suspect this clade D to be the uncertain species *S. bleekii* (*see* Discussion). Based on mitochondrial 16S, *S. incisa* individuals with fewer than 28 tentacles fell into two separate clades (B and C; Fig. 2). While the monophyly of both clades B and C containing *S. incisa* individuals with fewer than 28 tentacles was highly supported by bootstrap proportions and posterior probabilities, clades B and C were not inferred to be each other's closest relatives. The relationships of clades B and C to clade D suffered from low bootstrap support for 16S and missing taxon sampling for COI. Given the trimodal distribution of tentacle numbers (*see* previous section), *S. incisa* individuals were divided into < 28T and ≥ 28T morphotypes that may represent three species given the results of our phylogenetic analysis. Three additional *Solmissus* species/morphotypes were present within our occurrences dataset, namely *S. albescens* ($n = 16$; Supporting Information Fig. S13A), *S. marshalli* ($n = 4$; Supporting Information Fig. S13B), and an undescribed "nematocyst" morphotype ($n = 40$; Supporting Information Fig. S13C–E). As their

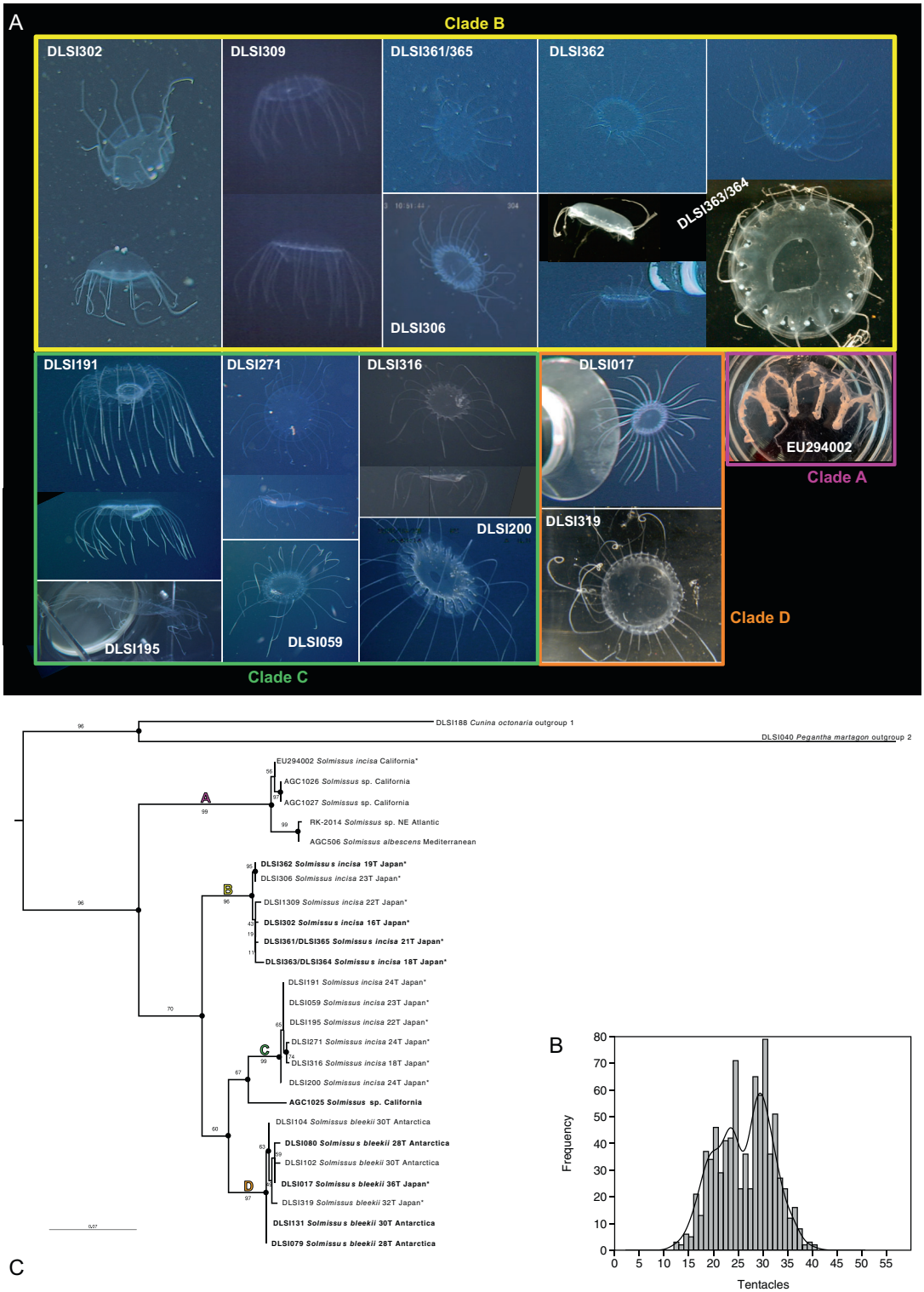

Fig. 2. (**A**) Photography of sequenced specimens, when available. The photographs were taken either from in situ videos by ROV or photographed once sampled. (**B**) Histogram of the number of tentacles for the observed "*Solmissus incisa*" individuals ($n = 814$). (**C**) Maximum likelihood phylogeny based on the mitochondrial marker 16S. Specimens of "*S. incisa*" of clade D were renamed as the (previously) uncertain species *S. bleekii*, which our study suggests is a valid species. Branch labels represent bootstrap proportions from 1000 non-parametric bootstraps; solid circles represent posterior probabilities > 0.95. Phylogenetic analyses were conducted under the GTR + G model. Tree labels include sample ID (*see* Supporting Information Table S2), species, number of tentacles (T) when available, and sampling area. Bold = sequenced both for 16S and COI, asterisk = photography provided.

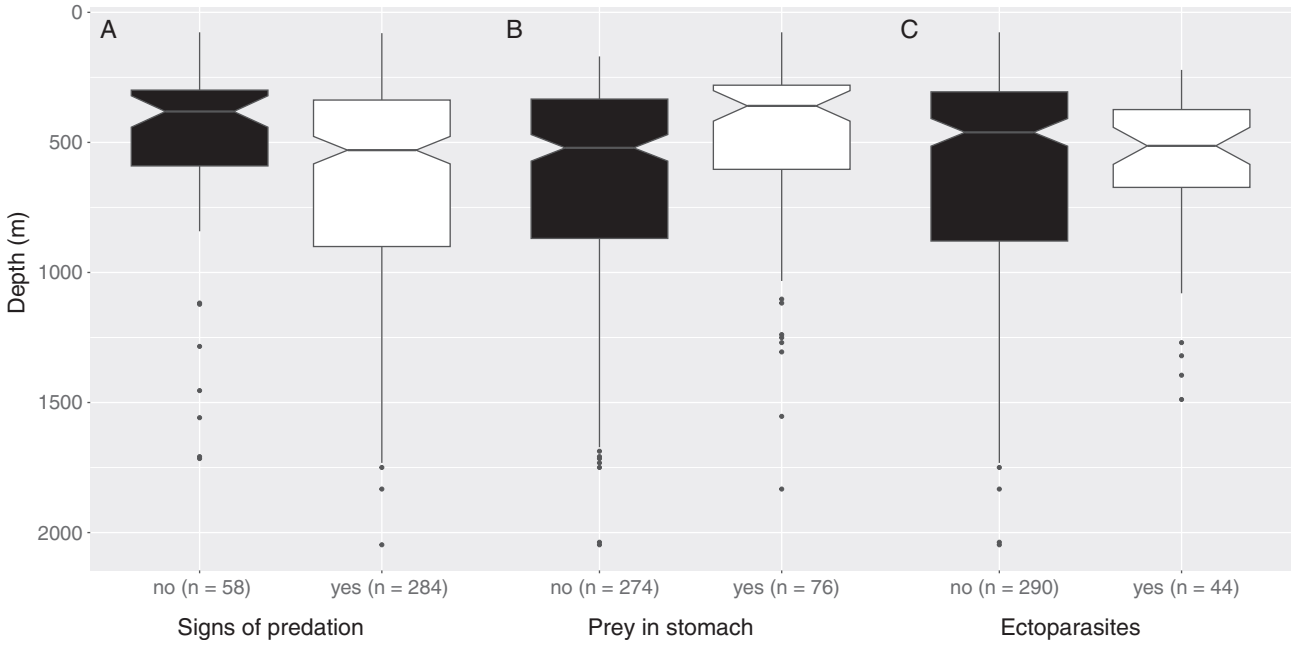

Fig. 3. Biotic factors ("signs of predation," "presence of prey in the stomach," and "presence of ectoparasites") related to depth. Significant differences are illustrated by non-overlapping notches (± 1.58 times the interquartile range divided by the square root of the number of observations).

presence data was insufficient for running ecological niche models at the putative species level, we only reported their occurrences in this study (Fig. 1B; Supporting Information Table S1).

Vertical migration

The diel vertical migration within our data was negligible, with no significant difference in depth between the occurrence data collected during daytime (median depth = 684.7 m, $n = 1259$) or nighttime (median depth = 670.9 m, $n = 124$) (Mann–Whitney $U = 76{,}270$, $z = 0.4213$, $p = 0.6736$) (Fig. 4A). Also within the morphotypes < 28T ($n_{day} = 500$, $n_{night} = 52$, median $depth_{day} = 461.9$ m, median $depth_{night} = 551.7$ m, Mann–Whitney $U = 12{,}150$, $z = 0.7761$, $p = 0.4377$) and ≥ 28T ($n_{day} = 440$, $n_{night} = 19$, median $depth_{day} = 851.7$ m, median $depth_{night} = 722.3$ m, Mann–Whitney $U = 3998.5$, $z = 0.3197$, $p = 0.7492$) there was no significant difference in vertical distribution between day or nighttime observations (Fig. 4B). Therefore, the dive time was ignored for all other analyses in this study.

Ecological niche modeling in 3D

Ecological niche models in 3D (Maxent and NOO3D) were first conducted for the genus *Solmissus* (OBIS dataset vs. our own compiled dataset), and then separately for the "*S. incisa*" morphotypes < 28T and ≥ 28T. Model performance metrics are given in Supporting Information Table S6. For the Maxent models, the threshold-independent metrics scored very well, with all test AUC ≥ 93.6%, and all CBI ≥ 0.796, except for the OBIS dataset which resulted in mediocre scores (test AUC = 86.1%, CBI = 0.684). The NOO3D models (resulting in discrete presence distribution maps only) performed well, with all pseudo-AUCs being at least 88.0% (excluding the OBIS model).

The distribution maps at different depths for *Solmissus* spp. with our compiled dataset for Maxent (probability of occurrences) and NOO3D (presence maps) are given in Supporting Information Fig. S14. Both models found the genus *Solmissus* to be predominantly present in the Northern Pacific, especially between the depths 400 and 1200 m, although lower (probabilities of) occurrences were also found at lower latitudes in the Atlantic and Indian oceans, whereas very low probabilities of occurrences to no occurrences were found in the Southern and Arctic oceans, respectively. When comparing the Maxent distribution maps for *Solmissus* spp. from the OBIS dataset vs. our compiled occurrences dataset (Supporting Information Fig. S15), the predicted distribution based on the OBIS dataset is much more widespread in the three dimensions, with much higher presence probabilities in shallower waters and the southern hemisphere. The distribution maps of the morphotypes < 28T and ≥ 28T are given in Fig. 5 for Maxent and in Supporting Information Fig. S16 for NOO3D. Here, the distribution resembles those of the genus *Solmissus*, except for division along the depth gradient, and the morphotype ≥ 28T is more likely to occur in deeper waters compared to the morphotype < 28T. This depth difference was more pronounced in the Maxent models than in the NOO3D models. The morphotype < 28T had a low probability of presence in the Atlantic and Indian oceans, whereas the morphotype ≥ 28T was nearly completely absent from latitudes

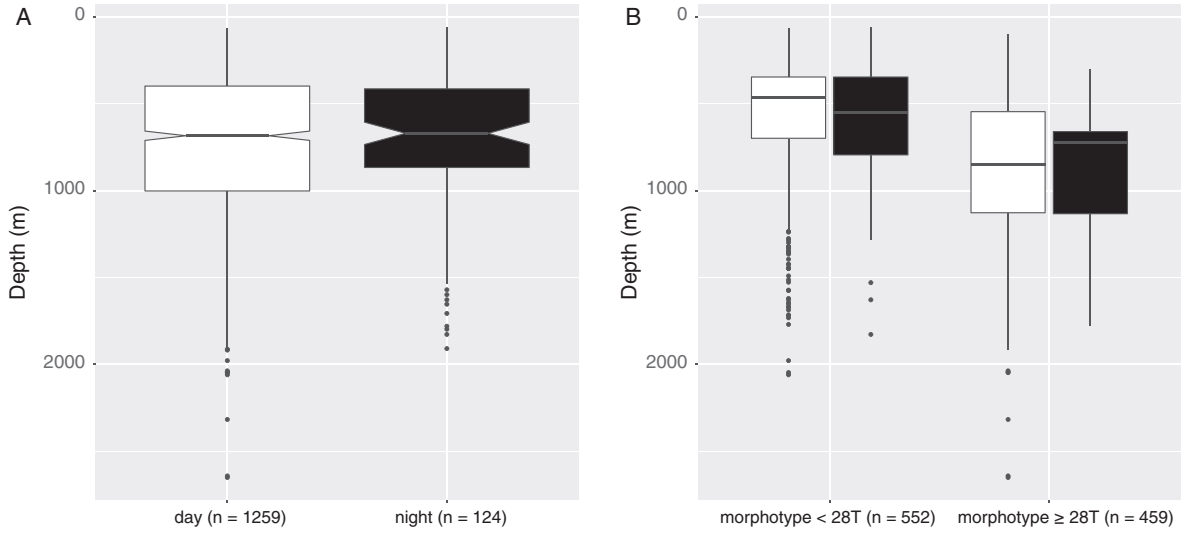

Fig. 4. Vertical distribution for all *Solmissus* spp. (**A**) and the morphotypes "less than 28 tentacles" (< 28T) and "more than or equal to 28 tentacles" (≥ 28T) (**B**). Boxplots show the median (middle line), quartiles (boxes), 1.5 times the interquartile range (whiskers), and extreme values (dots). Non-significant differences are illustrated by overlapping notches (± 1.58 times the interquartile range divided by the square root of the number of observations). White = daytime, black = nighttime.

north of 15°N in the Atlantic or within the southern hemisphere part of the Indian Ocean.

The relative contribution of each environmental variable to the 3D ecological niche models is illustrated in Fig. 6 and the values are given in Supporting Information Table S7. For all seven models, dissolved oxygen contributed the most, with values varying between 43.7% and 69.9%. Salinity was the second highest contributor to all NOO3D models and the OBIS Maxent model, whereas, for all the other Maxent models, its contribution was similar to depth. For Maxent, all four variables contributed to the models, whereas only three contributing environmental variables were found for NOO3D, with depth not contributing to the distribution of *Solmissus* spp. and the ≥ 28T morphotype, and temperature not contributing to the distribution of the < 28T morphotype.

The response curves of the presence probability for the genus *Solmissus* (OBIS vs. compiled occurrences dataset), and the morphotypes < 28T and ≥ 28T to those four environmental variables obtained with Maxent are given in Fig. 7. All modeled *Solmissus* groups, except for OBIS, showed similar response curves to the environmental variables, with only slight variations in the peak of their maximum presence probabilities or in the flatness of the curve (i.e., specificity of the ecological niche). The peak of probabilities was the highest for very low values of dissolved oxygen (c. 10 μmol kg^{-1}) and a salinity of 34. A shift in peak presence probabilities for depth and temperature was observed, with the < 28T found in shallower (c. 400 m) and warmer waters (c. 6°C) compared to the ≥ 28T (depth = c. 750 m, temperature = c. 3°C). The least performant model, based on the OBIS dataset, found the highest probability of occurrence for *Solmissus* spp. to be in shallower waters and for a wide range of temperatures.

Reproduction

Individuals of the genus *Solmissus* within the Northern Hemisphere were found to reproduce (i.e., individuals with visible oocytes/opaque spheres) all year round with no significant difference among seasons (Table 2; Supporting Information Fig. S17A), and an average of 38.4% reproducing individuals per season. Similar results were found for the morphotypes < 28T and ≥ 28T (Table 2; Supporting Information Fig. S17B,C). However, tentacle number was correlated with the reproduction of *Solmissus* (Table 2), with reproducing individuals generally having fewer tentacles (median = 26) compared to non-reproducing individuals (median = 28). As the depth and the CTD variables showed strong multicollinearity (Supporting Information Fig. S18), their effects on reproduction were tested in four distinct Mann–Whitney tests for equal medians (Table 2). The reproduction of individuals of the genus *Solmissus* was influenced by depth and temperature, but not by salinity or dissolved oxygen. Reproducing *Solmissus* spp. individuals were found in shallower and warmer waters compared to non-reproducing specimens. A similar effect on reproduction by depth and temperature, but not dissolved oxygen, was found for the two *Solmissus* tentacle morphotypes, except for salinity which had an effect on reproduction for the ≥ 28T morphotype but not the < 28T morphotypes. This time as well, reproducing individuals were found in shallower and warmer waters, and in slightly fresher waters for the ≥ 28T morphotype, in comparison to non-reproducing individuals (Table 2).

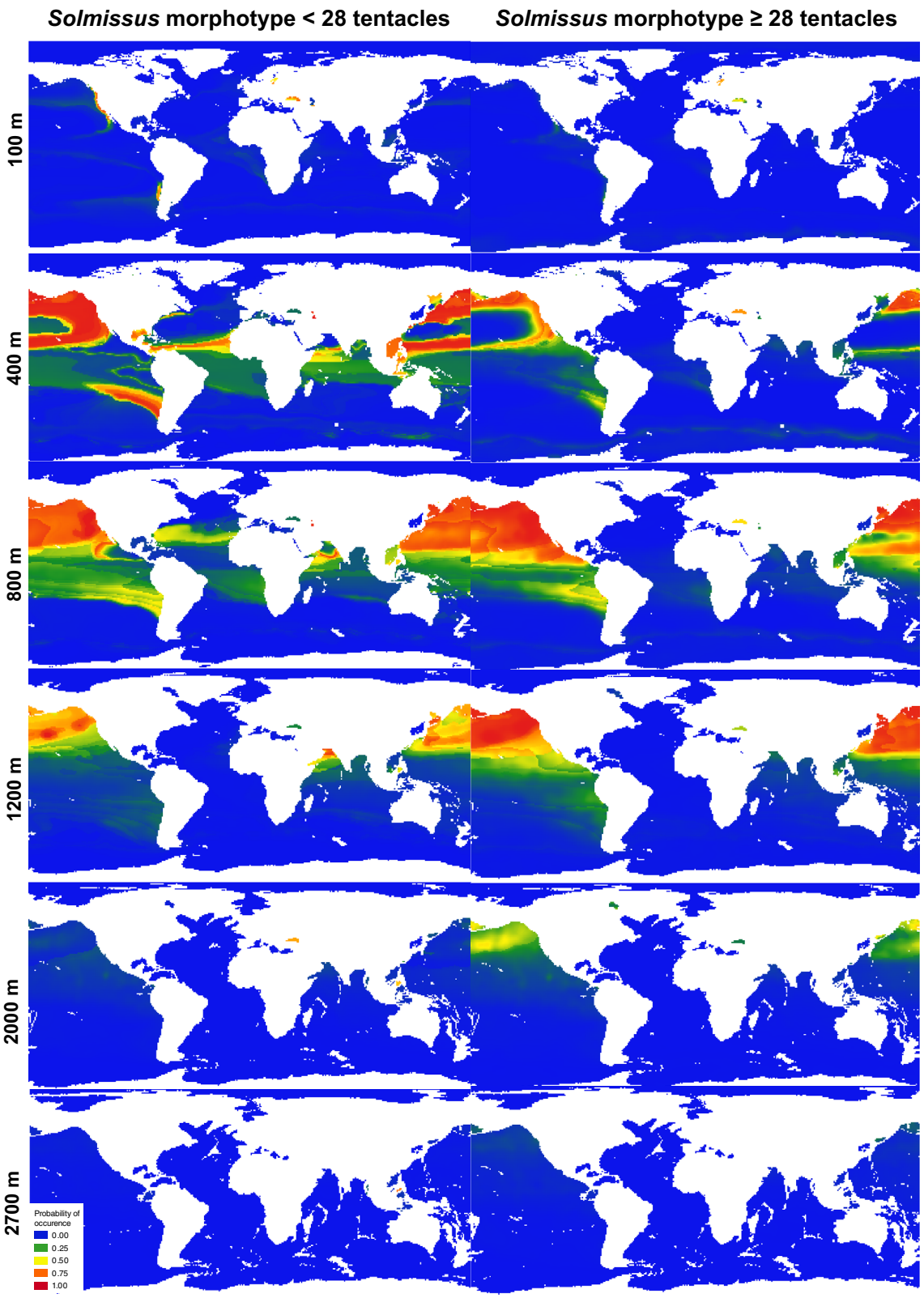

Fig. 5. Distribution maps at different depths for the *Solmissus* morphotypes "less than 28 tentacles" (left) and "more than or equal to 28 tentacles" (right). The maps were obtained by projecting the Maxent models and representing the probability of occurrence.

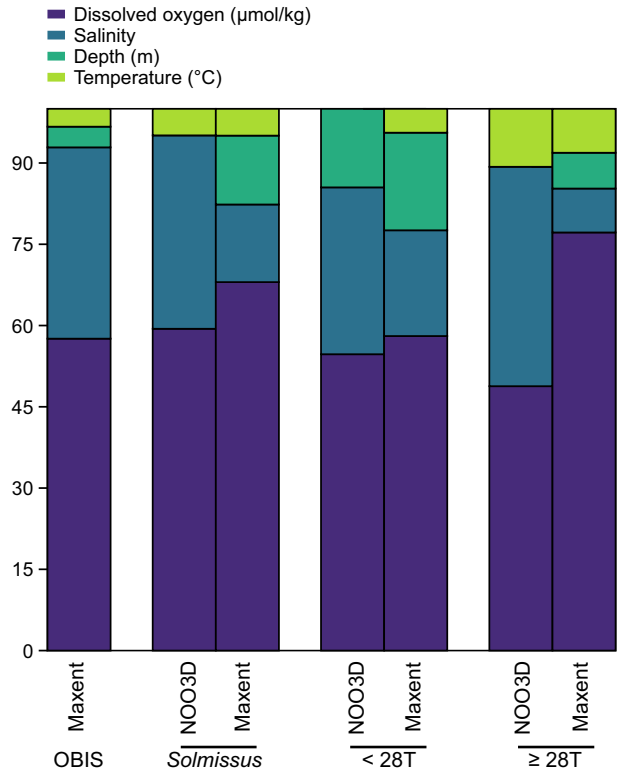

Fig. 6. Contribution (in %) of depth and the World Ocean Atlas 2018 environmental variables to the ecological niche models in 3D (NOO3D and Maxent) for the genus *Solmissus* (OBIS vs. our own compiled occurrences dataset), and the *Solmissus* morphotypes "less than 28 tentacles" (< 28T) and "more than or equal to 28 tentacles" (≥ 28T).

Discussion

Hidden diversity and its drivers

Our hypothesis that *S. incisa* represents a complex of several cryptic species (Toyokawa et al. 1998; Lindsay et al. 2015) was supported by our phylogenetic analyses. We detected at least three of these *S. incisa* cryptic species clades: two Japanese clades (B and C) with the number of tentacles varying between 16 and 24, and a widespread clade (D) found, at least, in waters off Japan, the North West Atlantic and the Eastern Antarctic, with tentacle numbers between 28 and 36. We suspect the latter to be the uncertain species *S. bleekii* which was described by Haeckel (1879) based on a specimen collected off the Atlantic coast of South Africa. This specimen was 40 mm wide, 10 mm high, biconvex, with rectangular gastric pouches, and rectangular lappets, twice as long as wide, each with one statocyst, but most importantly the specimen had 32 tentacles (Haeckel 1879). We, therefore, suggest that the individual GQ120083 identified as *S. incisa* by Ortman et al. (2010) is likely *S. bleekii* (*see* the COI phylogenetic tree; Supporting Information Fig. S12). In clade A, a specimen of *S. albescens* (AGC506) was closely related to a North East Atlantic *Solmissus* specimen (RK-2014). This could mean that *S. albescens* is perhaps not restricted to the Mediterranean Sea, or that the specimen AGC506 was misidentified, though at present the only *Solmissus* species yet reported from the Mediterranean Sea is *S. albescens* so the former hypothesis seems more likely. Individuals collected off California formed a monophyletic clade with *S. albescens*, suggesting that the Mediterranean and North East Atlantic population may in fact be a subspecies of a more widely distributed cryptic species. Although poorly supported by the bootstrap values, another Californian specimen (AGC1025) seemed closely related to clade C, potentially indicating even more hidden diversity. In summary, our phylogenetic results found that the genus *Solmissus* is more diverse than previously thought. Also, the geographic distribution of these species clades can be widespread, with potential spatial overlap. Clades with restricted distribution could reflect under-sampling. This shows that well-known cosmopolitan jellyfish "species" may be complexes of cryptic species, as also recently confirmed for other gelatinous taxa [e.g., the moon jellyfish *Aurelia* spp. (Lawley et al. 2021), and four-tentacled Narcomedusae previously identified as *Aegina citrea* (Lindsay et al. 2017)]. However, we only had both genetic markers investigated (16S and COI) for eight individuals. Further sampling, phylogenetic analyses, and an in-depth taxonomic study to define diagnostic characters are needed, as well as the inclusion of more specimens [e.g., the "nematocysts" morphotype (Supporting Information Fig. S13) and *Solmissus* spp. from the Southern Hemisphere (except for Eastern Antarctica)]. Although most of the OBIS observations of *Solmissus* spp. were from Monterey Bay's Video Annotation and Reference System database (87%), there are currently no molecular data for ROV-caught animals in pristine condition from that region.

Our hypothesis that differentiation within the genus *Solmissus* was driven by differences in geographic and environmental niches was partially supported. While our < 28T morphotype comprises multiple species, the ≥ 28T morphotype appears to represent a single species, *S. bleekii* (based on our restricted phylogenetic dataset). This ≥ 28T morphotype was predicted to be nearly fully absent in the Atlantic Ocean (north of 15°N) and the southern part of the Indian Ocean, compared to a low probability in these regions for the < 28T morphotype. More data are needed to find if this reflects sampling bias in the 2D space as, for instance, we had occurrence data for both morphotypes in the Atlantic Ocean. Our study had, however, enough data to support the hypothesis that different niches occurred along a vertical gradient, with both morphotypes showing similar responses to the tested environmental drivers, except for depth. This demonstrated again the importance of including the third dimension when modeling the distribution of pelagic species (Bentlage et al. 2013; Duffy and Chown 2017). Although there was some overlap, the < 28T morphotype (median $\text{depth}_{\text{day}} = 461.9$ m) was found in shallower waters compared to the ≥ 28T morphotype (median $\text{depth}_{\text{day}} = 851.7$ m). Here, we consider depth as a driver in

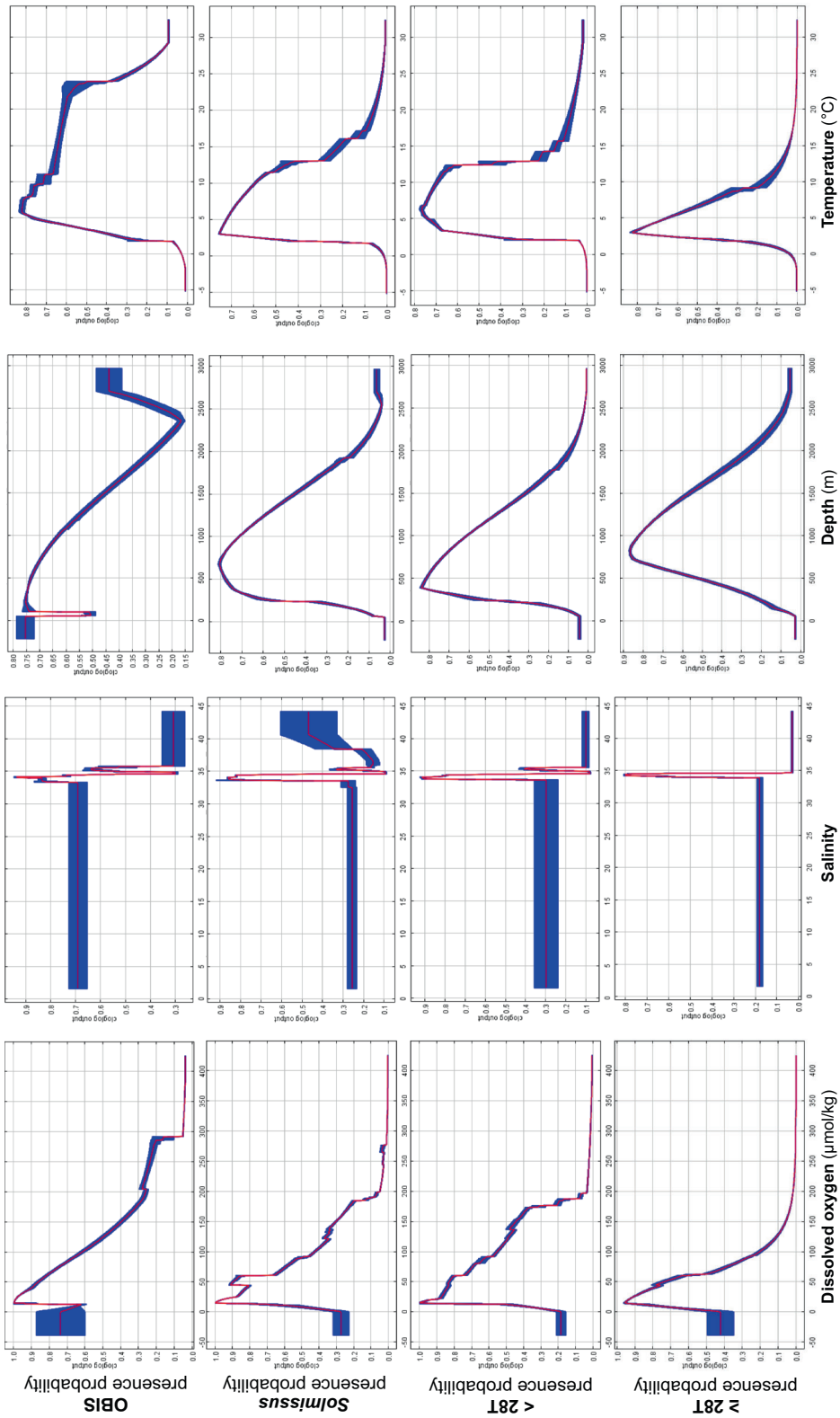

Fig. 7. Response curves showing the effects of depth and the World Ocean Atlas 2018 environmental variables on the presence predictions obtained by the 3D Maxent ecological niche models for the genus *Solmissus* (OBIS dataset vs. compiled dataset), and the "*S. incisa*" morphotypes "less than 28 tentacles" (< 28T) and "more than or equal to 28 tentacles" (≥ 28T). The response curves represent each different Maxent model per corresponding environmental variable.

Table 2. Results of the χ^2 and Mann–Whitney tests for equal medians testing differences in variables between reproducing and non-reproducing individuals for the whole genus *Solmissus*, and the morphotypes "less than 28 tentacles" (< 28T) and "more than or equal to 28 tentacles" (≥ 28T).

χ^2 tests		*n*	χ^2	df	*p*
Season	*Solmissus*	486	2.911	3	0.4055
	< 28T	236	3.9303	3	0.2691
	≥ 28T	244	2.112	3	0.5495

Mann–Whitney tests		*n*	*U*	*z*	*p*	Median reproducing vs. non-reproducing	
Tentacles	*Solmissus*	486	17,880	2.1984	**0.0271***	*26*	*28*
Depth (m)	*Solmissus*	370	12,577	2.8113	**0.0049***	420.47	543.2
	< 28T	171	2596.5	2.1364	**0.0326***	350.65	434.14
	≥ 28T	193	3385	2.1118	**0.0347***	507.38	701.06
Temperature (°C)	*Solmissus*	370	12,444	2.9474	**0.0032***	6.788	6.127
	< 28T	171	2473	2.5411	**0.0111***	7.46	6.87
	≥ 28T	193	3412.5	2.0368	**0.0417***	6.18	4.93
Salinity (PSU)	*Solmissus*	370	13,388	1.9201	0.0548	No significant difference	
	< 28T	171	3091	04258	0.6702	No significant difference	
	≥ 28T	193	3347.5	2.214	**0.0268***	34.24	34.33
Dissolved oxygen (mL L^{-1})	*Solmissus*	370	13,571	1.7898	0.0735	No significant difference	
	< 28T	171	2809.5	1.4385	0.1503	No significant difference	
	≥ 28T	193	3902.5	0.7008	0.4835	No significant difference	

Note: Significant *p* values ($p < 0.05$) are highlighted with an asterisk.

differentiation and speciation processes. Although vertical speciation has been less demonstrated so far in holoplanktonic species compared to benthic ones, other likely midwater jellyfish examples include the genera *Erenna* (Pugh and Haddock 2016) and *Botrynema* (Larson 1986; Montenegro et al. 2023). It is unknown why specimens with more tentacles are found in deeper waters but it is unlikely to be related to reproduction since both shallower and deeper morphotypes were shown to reproduce all year round. Neither can we point to a biotic effect as we found no link between tentacle number and signs of predation, presence of prey in the stomach of the jellyfish, or ectoparasites. However, perhaps tentacle number still reflects an adaption to different prey types. More tentacles at the same disk diameter would allow them to feed on smaller animals and be more efficient at catching prey due to the increased probability of a prey item coming in contact with a tentacle within a given volume the medusa was swimming through. Salps are common prey items of *Solmissus* and their chains are more often encountered in shallower waters (Choy et al. 2017). Even with fewer tentacles, at least one tentacle would be expected to come in contact somewhere along the chain, while in deeper waters individual medusae are more common as prospective food items than salp chains and more tentacles would translate into higher predation success.

Ecology and distribution

Contrary to our hypothesis, we found the modeled distribution of the genus *Solmissus* and the two tentacle morphotypes was mostly driven by dissolved oxygen and salinity, and slightly by depth and temperature. Temperature, depth, and to a lesser extent salinity, are well-known drivers of the distribution of hydromedusae in general (e.g., Raskoff 2001; Hoving et al. 2020; Mańko et al. 2020), as well as in epipelagic Californian (Luo et al. 2014) and midwater Arctic Narcomedusae (Pantiukhin et al. 2023). Dissolved oxygen was also found to have an effect on the distribution of Californian (Luo et al. 2014) and Cape Verdean Narcomedusae (Hoving et al. 2020). The preferred dissolved oxygen concentration range of Narcomedusae has, however, been reported to be species-specific, with some species found at low concentrations or in the oxygen minimum zone (Luo et al. 2014; Hoving et al. 2020). Our ecological niche models found a distribution of *Solmissus* spp. that roughly followed the global oxygen minimum zones (Moffitt et al. 2015) with the highest presence probability of *Solmissus* spp. at dissolved oxygen values of c. 10 μmol kg^{-1}, which correspond to the "severe hypoxia" and "oxygen minimum zone" thresholds according to Diaz and Rosenberg (2008). In the epipelagic, this hypoxia tolerance of medusae and their polyps, combined with their ability to quickly "bloom" in response to food availability, makes jellyfish especially well equipped to flourish in eutrophic habitats to the detriment of other invertebrate taxa or fish (Purcell et al. 2001). Tolerance to hypoxia can be partly explained by low metabolic rates and the capacity for oxygen storage in the mesoglea of jellyfish (Thuesen and Childress 1994; Thuesen et al. 2005). As oceans are currently

facing global deoxygenation (Schmidtko et al. 2017), with oxygen minimum zones expanding (Moffitt et al. 2015), our findings suggest that *Solmissus* spp. will not only withstand, but may be able to also expand, its distribution and ecological impact as other marine organisms are threatened by changing oxygen conditions. As Narcomedusae feed on a high diversity of deep pelagic gelatinous prey (Raskoff 2002; Choy et al. 2017), this may impact the whole midwater food web.

Recently, efforts to characterize marine pelagic biogeographic regions have increased (e.g., Sherman 1991; Sutton et al. 2017). Jellyfish (e.g., Abboud et al. 2018) or other taxa such as mesopelagic fishes (e.g., Freer et al. 2022), however, can display broad spatial distributions that encompass multiple regions. This is especially the case for holoplanktonic medusae, which are more globally distributed compared to meroplanktonic species (Boosten et al. 2023), and therefore must show greater tolerance to a range of biotic and abiotic factors. Such wide distribution and high tolerance are what we observed for the holoplanktonic *Solmissus* spp. Low oxygen extremes were the strongest environmental drivers for some mesopelagic ecoregions (Sutton et al. 2017), and while taxa such as the hyper-diverse lanternfish family were generally absent from these regions (Freer et al. 2022), this is where we found the highest presence probability for *Solmissus* spp. All these marine ecoregions, however, have been delimited on a 2D global scale, and no characterization for the rest of the midwater, under the mesopelagic zone, exists. As we found depth to be a major driver in determining the distribution of our different morphotypes, to understand biogeographic midwater processes, we highly recommend that in the future, midwater ecoregions are delimited as 3D spaces.

Sampling bias and the importance of online biogeographic databases

Online biographic databases are extremely valuable to study midwater ecosystems. Previous case studies have already demonstrated the importance of citizen-derived databases for studying epipelagic jellyfish (e.g., Pikesley et al. 2014; Anthony et al. 2023). In this study, we further show the importance of online biogeographic databases, especially when including imagery or videography, which allowed for testing ecological and evolutionary hypotheses related to different morphotypes, biotic interactions, and reproduction, but also resulted in higher performing ecological niche models. The majority of our *Solmissus* spp. data came from the Northern Pacific, where they were collected down to a depth of 2700 m. It is possible that with additional and deeper surveys, *Solmissus* may be found in even deeper waters and potentially even at hadal depths (e.g., Jamieson et al. 2023). Our study shows an additional sampling bias in the 2D space, especially for records including morphological information. Despite us pruning out the North Pacific presence data and target-group background points not resulting in better scoring models, it seems that this sampling bias is reflected in their outputs, which need to be assessed carefully. For instance, Youngbluth et al. (2008) found *Solmissus* to occur during all 14 ROV dives near the mid-Atlantic Ridge in July 2004 with sightings between 279 and 1333 m depth but with 51% (50 individuals) occurring between 500 and 700 m depth. Both our Maxent and NOO3D projections predicted a low probability of occurrence for *Solmissus* in this area (Fig. 5; Supporting Information Fig. S5, S6). Our models also predicted a higher probability of occurrences for *Solmissus* spp. in locations with no known observations, such as the Baltic and Caspian seas, likely due to their low dissolved oxygen concentrations. Despite these caveats, ecological niche modeling remains a cost-effective way to assess distribution and ecological patterns (Domisch et al. 2017), especially for vast and hard-to-sample biomes such as the midwater. Most of our data was also collected during the daytime, and as a result, the lack of vertical migration detected within our dataset could reflect this sampling bias as well. With mesopelagic zooplankton being well-known for their diel vertical migration (Brierley 2014), it would certainly be beneficial to conduct more nighttime collections in the future, especially given that the congener *S. albescens* is a well-known diel vertical migrator (Mills and Goy 1988).

Reproduction

Solmissus spp. were reproducing all year round, similar to the midwater jellyfishes *Atolla* spp. and *Periphylla periphylla* (Larson 1986; Jarms et al. 1999; Lucas and Reed 2009). Our hypothesis that reproduction was driven by temperature and salinity was partially supported. We found reproducing *Solmissus* spp. all in shallower and warmer waters compared to non-reproducing ones. As depth was correlated with temperature, we cannot distinguish if reproduction was influenced by depth and/or temperature. The association between temperature and reproduction has long been demonstrated for a variety of zooplankton taxa, including jellyfish (Rossi et al. 2019; Mańko et al. 2022). Higher temperatures within the thermal optima of species often result in earlier reproduction and faster development (Beaugrand and Kirby 2018; Rossi et al. 2019). As most deep-sea species live in very stable thermal regimes, warming up to 1°C may exert stress, cause range shifts, or alter species interactions (Levin and Le Bris 2015). However, the difference in temperature between reproducing and not-reproducing *Solmissus* specimens was up to 1.25°C for the ≥ 28T morphotype, suggesting that the estimated ocean warming in deep basins of up to 0.1°C per decade (although with some spatial heterogeneity) (Purkey and Johnson 2010) might favor the reproduction of *Solmissus* spp. No effect of the biotic factors on reproduction was found.

Conclusion

Narcomedusae play key roles in the midwater ecosystem as top-down regulators. Using ecological niche modeling in 3D, we found that a common widespread narcomedusa, *Solmissus*

spp., will likely respond to ongoing ocean changes by expanding its distribution, which was highly correlated to low dissolved oxygen values, and reproducing more since reproducing individuals are found in slightly warmer waters. Our phylogenetic analyses revealed hidden diversity within the *Solmissus* genus, with different tentacle morphotypes occupying different optimal vertical niches. Our study demonstrated the importance of interdisciplinary studies to answer evolutionary and ecological questions about widespread midwater jellyfish. Our study further illustrated the value of online biogeographic databases, especially when they include imagery and videography records, for studying midwater organisms and treating midwater biogeographic regions as 3D spaces.

Data availability statement

All new sequences were deposited at NCBI GenBank (for accession numbers *see* Supporting Information Table S2) and previously unpublished photographs of *Solmissus* are available at http://morphobank.org/permalink/?P4437 (*see* Supporting Information Table S1 for metadata).

References

Abboud, S. S., L. G. Daglio, and M. N. Dawson. 2018. A global estimate of genetic and geographic differentiation in macromedusae—implications for identifying the causes of jellyfish blooms. Mar. Ecol. Prog. Ser. **591**: 199–216. doi:10.3354/meps12521

Anthony, C. J., K. C. Tan, K. A. Pitt, B. Bentlage, and C. L. Ames. 2023. Leveraging public data to predict global niches and distributions of Rhizostome jellyfishes. Animals **13**: 1591. doi:10.3390/ani13101591

Barber, R. A., S. G. Ball, R. K. A. Morris, and F. Gilbert. 2020. Target-group backgrounds prove effective at correcting sampling bias in maxent models. Divers. Distrib. **28**: 128–141. doi:10.1111/ddi.13442

Bates, D., M. Mächler, B. Bolker, and S. Walker. 2015. Fitting linear mixed-effects models using *lme4*. J. Stat. Softw. **67**: 1–48. doi:10.18637/jss.v067.i01

Beaugrand, G., and R. R. Kirby. 2018. How do marine pelagic species respond to climate change? Theories and observations. Ann. Rev. Mar. Sci. **10**: 169–197. doi:10.1146/annurev-marine-121916-063304

Bentlage, B., A. T. Peterson, N. Barve, and P. Cartwright. 2013. Plumbing the depths: Extending ecological niche modelling and species distribution modelling in three dimensions. Glob. Ecol. Biogeogr. **22**: 952–961. doi:10.1111/geb.12049

Bentlage, B., K. J. Osborn, D. J. Lindsay, R. R. Hopcroft, K. A. Raskoff, and A. G. Collins. 2018. Loss of metagenesis and evolution of a parasitic life style in a group of open-ocean jellyfish. Mol. Phylogenet. Evol. **124**: 50–59. doi:10.1016/j.ympev.2018.02.030

Boosten, M., C. Sant, O. Da Silva, S. Chaffron, L. Guidi, and L. Leclère. 2023. Loss of the benthic life stage in Medusozoa and colonization of the open ocean. bioRxiv, 2023.02.15.528668. doi:010.1101/2023.02.15.528668

Bouillon, J., C. Gravili, F. Pagès, J.-M. Gili, and F. Boero. 2006. An introduction to hydrozoa, v. **194**. Mémoires du Muséum national d'Histoire naturelle, p. 1–591.

Boyce, M. S., P. R. Vernier, S. E. Nielsen, and F. K. A. Schmiegelow. 2002. Evaluating resource selection functions. Ecol. Model. **157**: 281–300. doi:10.1016/S0304-3800(02)00200-4

Brierley, A. S. 2014. Diel vertical migration. Curr. Biol. **24**: R1074–R1076. doi:10.1016/j.cub.2014.08.054

Castresana, J. 2000. Selection of conserved blocks from multiple alignments for their use in phylogenetic analysis. Mol. Biol. Evol. **17**: 540–552. doi:10.1093/oxfordjournals.molbev.a026334

Choy, C. A., S. H. D. Haddock, and B. H. Robison. 2017. Deep pelagic food web structure as revealed by *in situ* feeding observations. Proc. Biol. Sci. **284**: 20172116. doi:10.1098/rspb.2017.2116

Cunningham, C. W., and L. W. Buss. 1993. Molecular evidence for multiple episodes of paedomorphosis in the family Hydractiniidae. Biochem. Syst. Ecol. **21**: 57–69. doi:10.1016/0305-1978(93)90009-G

Darriba, D., G. L. Taboada, R. Doallo, and D. Posada. 2012. jModelTest 2: More models, new heuristics and parallel computing. Nat. Methods **9**: 772. doi:10.1038/nmeth.2109

Diaz, R. J., and R. Rosenberg. 2008. Spreading dead zones and consequences for marine ecosystems. Science **321**: 926–929. doi:10.1126/science.1156401

Domisch, S., and others. 2017. Modelling approaches for the assessment of projected impacts of drivers of change on biodiversity, ecosystems functions and aquatic ecosystems service delivery. Aquacross Deliverable 7.1. doi:10.13140/RG.2.2.30105.72800

Dormann, C. F., and others. 2013. Collinearity: A review of methods to deal with it and a simulation study evaluating their performance. Ecography **36**: 27–46. doi:10.1111/j.1600-0587.2012.07348.x

Drazen, J. C., and others. 2020. Midwater ecosystems must be considered when evaluating environmental risks of deep-sea mining. Proc. Natl. Acad. Sci. USA **117**: 17455–17460. doi:10.1073/pnas.2011914117

Duffy, G. A., and S. L. Chown. 2017. Explicitly integrating a third dimension in marine species distribution modelling. Mar. Ecol. Prog. Ser. **564**: 1–8. doi:10.3354/meps12011

Folmer, O., M. Black, W. Hoeh, R. Lutz, and R. Vrijenhoek. 1994. DNA primers for amplification of mitochondrial cytochrome *c* oxidase subunit I from diverse metazoan invertebrates. Mol. Mar. Biol. Biotechnol. **3**: 294–299.

Fox, J., and S. Weisberg. 2011. An R companion to applied regression, 2nd ed. Sage.

Freer, J. J., G. A. Tarling, M. A. Collins, J. C. Partridge, and M. J. Genner. 2020. Estimating circumpolar distribution of lanternfish using 2D and 3D ecological niche models. Mar. Ecol. Prog. Ser. **647**: 179–193. doi:10.3354/meps13384

Freer, J. J., R. A. Collins, G. A. Tarling, M. A. Collins, J. C. Partridge, and M. J. Genner. 2022. Global phylogeography of hyperdiverse lanternfishes indicates sympatric speciation in the deep sea. Glob. Ecol. Biogeogr. **31**: 2353–2367. doi:10.1111/geb.13586

García-Roselló, E., C. Guisande, L. González-Vilas, J. González-Dacosta, J. Heine, E. Pérez-Costas, and J. M. Lobo. 2019. A simple method to estimate the probable distribution of species. Ecography **42**: 1613–1622. doi:10.1111/ecog.04563

Gasca, R., E. Suárez-Morales, and S. H. D. Haddock. 2007. Symbiotic associations between crustaceans and gelatinous zooplankton in deep and surface waters off California. Mar. Biol. **151**: 233–242. doi:10.1007/s00227-006-0478-y

Gasca, R., R. Hoover, and S. H. D. Haddock. 2015. New symbiotic associations of hyperiid amphipods (Peracarida) with gelatinous zooplankton in deep waters off California. J. Mar. Biol. Assoc. **95**: 503–511. doi:10.1017/S0025315414001416

Garcia, H. E., and others. 2018. World Ocean Atlas 2018, Volume 3: Dissolved Oxygen, Apparent Oxygen Utilization, and Oxygen Saturation. A. Mishonov Technical Ed. NOAA Atlas NESDIS 83: 38.

Genzano, G., H. Mianzan, and J. Bouillon. 2008. Hydromedusae (Cnidaria: Hydrozoa) from the temperate southwestern Atlantic Ocean: A review. Zootaxa **1750**: 1–18. doi:10.11646/zootaxa.1750.1.1

Haddock, S. H. D., and J. F. Case. 1999. Bioluminescence spectra of shallow and deep-sea gelatinous zooplankton: Ctenophores, medusae and siphonophores. Mar. Biol. **133**: 571–582. doi:10.1007/s002270050497

Haeckel, E. H. P. A. 1879. Monographie der Medusen. G. Fischer.

Hammer, Ø., D. A. T. Harper, and P. D. Ryan. 2001. PAST—PAlaeontological STatistics. Paleontologia Electronica 1–9.

Hartman, O., and K. O. Emery. 1956. Bathypelagic coelenterates. Limnol. Oceanogr. **1**: 304–312. doi:10.4319/lo.1956.1.4.0304

Hidaka-Umetsu, M., and D. J. Lindsay. 2018. First record of the mesopelagic narcomedusan genus *Solmissus* ingesting a fish, with notes on morphotype diversity in *S. incisa* (Fewkes, 1886). Plankton Benthos Res. **13**: 41–45. doi:10.3800/pbr.13.41

Hoving, H. J., and others. 2019. The Pelagic In situ Observation System (PELAGIOS) to reveal biodiversity, behavior, and ecology of elusive oceanic fauna. Ocean Sci. **15**: 1327–1340. doi:10.5194/os-15-1327-2019

Hoving, H. J. T., P. Neitzel, H. Hauss, S. Christiansen, R. Kiko, B. H. Robison, P. Silva, and A. Körtzinger. 2020. In situ observations show vertical community structure of pelagic fauna in the eastern tropical North Atlantic off Cape Verde. Sci. Rep. **10**: 21798. doi:10.1038/s41598-020-78255-9

Huelsenbeck, J. P., and F. Ronquist. 2001. MRBAYES: Bayesian inference of phylogenetic trees. Bioinformatics **17**: 754–755. doi:10.1093/bioinformatics/17.8.754

Hutchinson, G. E. 1957. Concluding remarks. In Cold Spring Harbour Symposium on Quantitative Biology. 415–427.

Jacobsen Stout, N., L. Kuhnz, L. Lundsten, B. Schlining, K. Schlining, and S. von Thun [eds.]. The Deep-Sea Guide (DSG). *In* Monterey Bay Aquarium Research Institute (MBARI). Consulted on: 2019-05-01.

Jamieson, A. J., D. J. Lindsay, and H. Kitazato. 2023. Maximum depth extensions for Hydrozoa, Tunicata and Ctenophora. Mar. Biol. **170**: 33. doi:10.1007/s00227-023-04177-5

Jarms, G., U. Båmstedt, H. Tiemann, M. B. Martinussen, J. H. Fosså, and T. Høisœter. 1999. The holopelagic life cycle of the deep-sea medusa *Periphylla periphylla* (Scyphozoa, Coronatae). Sarsia **84**: 55–65. doi:10.1080/00364827.1999.10420451

Jiménez-Valverde, A., J. M. Lobo, and J. Hortal. 2008. Not as good as they seem: The importance of concepts in species distribution modelling. Divers. Distrib. **14**: 885–890. doi:10.1111/j.1472-4642.2008.00496.x

Kass, J. M., R. Muscarella, P. J. Galante, C. L. Bohl, G. E. Pinilla-Buitrago, R. A. Boria, M. Soley-Guardia, and R. P. Anderson. 2021. ENMeval 2.0: Redesigned for customizable and reproducible modeling of species' niches and distributions. Methods Ecol. Evol. **12**: 1602–1608. doi:10.1111/2041-210X.13628

Katija, K., and others. 2022. FathomNet: A global image database for enabling artificial intelligence in the ocean. Sci. Rep. **12**: 15914. doi:10.1038/s41598-022-19939-2

Katoh, K., and D. M. Standley. 2013. MAFFT multiple sequence alignment software version 7: Improvements in performance and usability. Mol. Biol. Evol. **30**: 772–780. doi:10.1093/molbev/mst010

Kawamura, M., and S. Kubota. 2008. Influences of temperature and salinity on asexual budding by hydromedusa *Proboscidactyla ornata* (Cnidaria: Hydrozoa: Proboscidactylidae). J. Mar. Biol. Assoc. **88**: 1601–1606. doi:10.1017/S0025315408002944

Larson, R. J. 1986. Pelagic scyphomedusae (Scyphozoa: Coronatae and Semaeostomeae) of the Southern Ocean, p. 59–165. *In* L. S. Kornicker [ed.], Biology of the Antarctic seas. American Geophysical Union. doi:10.1002/9781118666579.ch3

Larson, R. J., C. E. Mills, and G. R. Harbison. 1989. In situ foraging and feeding behaviour of Narcomedusae (Cnidaria: Hydrozoa). J. Mar. Biol. Assoc. **69**: 785–794. doi:10.1017/S002531540003215X

Lawley, J. W., E. Gamero-Mora, M. M. Maronna, L. M. Chiaverano, S. N. Stampar, R. R. Hopcroft, A. G. Collins,

and A. C. Morandini. 2021. The importance of molecular characters when morphological variability hinders diagnosability: Systematics of the moon jellyfish genus *Aurelia* (Cnidaria: Scyphozoa). PeerJ **9**: e11954. doi:10.7717/peerj.11954

Levin, L. A., and N. Le Bris. 2015. The deep ocean under climate change. Science **350**: 766–768. doi:10.1126/science.aad0126

Levin, N., S. Kark, and R. Danovaro. 2018. Adding the third dimension to marine conservation. Conserv. Lett. **11**: e12408. doi:10.1111/conl.12408

Lindsay, D., M. Umetsu, M. Grossmann, H. Miyake, and H. Yamamoto. 2015. The gelatinous macroplankton community at the Hatoma Knoll hydrothermal vent, p. 639–666. *In* J. Ishibashi, K. Okino, and M. Sunamura [eds.], Subseafloor biosphere linked to hydrothermal systems. Springer. doi:10.1007/978-4-431-54865-2_51

Lindsay, D. J., and others. 2017. The perils of online biogeographic databases: A case study with the "monospecific" genus *Aegina* (Cnidaria, Hydrozoa, Narcomedusae). Mar. Biol. Res. **13**: 494–512. doi:10.1080/17451000.2016.1268261

Lucas, C. H., and A. J. Reed. 2009. Observations on the life histories of the narcomedusae *Aeginura grimaldii*, *Cunina peregrina* and *Solmissus incisa* from the western North Atlantic. Mar. Biol. **156**: 373–379. doi:10.1007/s00227-008-1089-6

Luo, J. Y., B. Grassian, D. Tang, J. O. Irisson, A. T. Greer, C. M. Guigand, S. McClatchie, and R. K. Cowen. 2014. Environmental drivers of the fine-scale distribution of a gelatinous zooplankton community across a mesoscale front. Mar. Ecol. Prog. Ser. **510**: 129–149. doi:10.3354/meps10908

Locarnini, R. A., and others. 2018. World Ocean Atlas 2018, Volume 1: Temperature. A. Mishonov Technical Ed. NOAA Atlas NESDIS 81: 52.

Mańko, M. K., M. Gluchowska, and A. Weydmann-Zwolicka. 2020. Footprints of Atlantification in the vertical distribution and diversity of gelatinous zooplankton in the Fram Strait (Arctic Ocean). Prog. Oceanogr. **189**: 102414. doi:10.1016/j.pocean.2020.102414

Mańko, M. K., M. Malgorzata, S. Kwasniewski, and A. Weydmann-Zwolicka. 2022. Atlantification alters the reproduction of jellyfish *Aglantha digitale* in the European Arctic. Limnol. Oceanogr. **67**: 1836–1849. doi:10.1002/lno.12170

Mills, C. E., and J. Goy. 1988. In situ observations of the behavior of mesopelagic *Solmissus* Narcomedusae (Cnidaria, Hydrozoa). Bull. Mar. Sci. **43**: 739–751.

Mills, C. E., P. R. Pugh, G. R. Harbison, and S. H. D. Haddock. 1996. Medusae, siphonophores and ctenophores of the Alboran Sea, south western Mediterranean. Sci. Mar. **60**: 145–163.

Moffitt, S. E., R. A. Moffitt, W. Sauthoff, C. V. Davis, K. Hewett, and T. M. Hill. 2015. Paleoceanographic insights on recent oxygen minimum zone expansion: Lessons for modern oceanography. PLoS One **10**: e0115246. doi:10.1371/journal.pone.0115246

Montenegro, J., and others. 2023. Heterogeneity in diagnostic characters across ecoregions: A case study with *Botrynema* (Hydrozoa: Trachylina: Halicreatidae). Front. Mar. Sci. **9**: 1101699. doi:10.3389/fmars.2022.1101699

Ortman, B. D., A. Bucklin, F. Pagès, and M. Youngbluth. 2010. DNA barcoding the Medusozoa using mtCOI. Deep-Sea Res. II: Top. Stud. Oceanogr. **57**: 2148–2156. doi:10.1016/j.dsr2.2010.09.017

Osborn, D. A. 2000. Cnidarian "parasites" on *Solmissus incisa*, a narcomedusa. Sci. Mar. **64**: 157–163. doi:10.3989/scimar.2000.64s1157

Pantiukhin, D., G. Verhaegen, C. Kraan, K. Jerosch, P. Neitzel, H.-J. Hoving, and C. Havermans. 2023. Optical observations and spatio-temporal projections of gelatinous zooplankton in the Fram Strait, a gateway to a changing Arctic Ocean. Front. Mar. Sci. **10**: 987700. doi:10.3389/fmars.2023.987700

Peres, J. M. 1959. Deux plongées au large du Japon avec le bathyscaphe français F.N.R.S. III. Bull. Inst. Océan. Monaco **1134**: 1–28.

Pérez-Costas, E., C. Guisande, L. González-Vilas, E. García-Roselló, J. Heine, J. González-Dacosta, and J. M. Lobo. 2019. NOO3D: A procedure to perform 3D species distribution models. Ecol. Inform. **54**: 101008. doi:10.1016/j.ecoinf.2019.101008

Phillips, S. J., R. P. Anderson, and R. E. Schapire. 2006. Maximum entropy modeling of species geographic distributions. Ecol. Model. **190**: 231–259. doi:10.1016/j.ecolmodel.2005.03.026

Phillips, S. J., 2017. A Brief Tutorial on Maxent. Accessed on 2018-12-10, available from url: https://biodiversityinformatics.amnh.org/open_source/maxent/Maxent_tutorial2017.pdf

Pikesley, S. K., B. J. Godley, S. Ranger, P. B. Richardson, and M. J. Witt. 2014. Cnidaria in UK coastal waters: Description of spatio-temporal patterns and inter-annual variability. J. Mar. Biol. Assoc. **94**: 1401–1408. doi:10.1017/S0025315414000137

Pugh, P. R., and S. H. D. Haddock. 2016. A description of two new species of the genus *Erenna* (Siphonophora: Physonectae: Erennidae), with notes on recently collected specimens of other *Erenna* species. Zootaxa **4189**: 401. doi:10.11646/zootaxa.4189.3.1

Purcell, J. E., D. L. Breitburg, M. B. Decker, W. M. Graham, M. J. Youngbluth, and K. A. Raskoff. 2001. Pelagic cnidarians and ctenophores in low dissolved oxygen environments: A review, p. 77–100. *In* N. N. Rabalais and R. E. Turner [eds.], Coastal hypoxia: Consequences for living resources and ecosystems. American Geophysical Union. doi:10.1029/CE058p0077

Purkey, S. G., and G. C. Johnson. 2010. Warming of global abyssal and deep Southern Ocean waters between the

1990s and 2000s: Contributions to global heat and sea level rise budgets. J. Clim. **23**: 6336–6351. doi:10.1175/2010JCLI3682.1

R Core Team. 2023. R: A language and environment for statistical computing. R Foundation for Statistical Computing, https://www.R-project.org/

Raskoff, K. A. 2001. The impact of El Niño events on populations of mesopelagic hydromedusae. Hydrobiologia **451**: 121–129. doi:10.1023/A:1011812812662

Raskoff, K. A. 2002. Foraging, prey capture, and gut contents of the mesopelagic narcomedusa *Solmissus* spp. (Cnidaria: Hydrozoa). Mar. Biol. **141**: 1099–1107. doi:10.1007/s00227-002-0912-8

Robinson, L. M., J. Elith, A. J. Hobday, R. G. Pearson, B. E. Kendall, H. P. Possingham, and A. J. Richardson. 2011. Pushing the limits in marine species distribution modelling: Lessons from the land present challenges and opportunities. Glob. Ecol. Biogeogr. **20**: 789–802. doi:10.1111/j.1466-8238.2010.00636.x

Robison, B. H. 2004. Deep pelagic biology. J. Exp. Mar. Biol. Ecol. **300**: 253–272. doi:10.1016/j.jembe.2004.01.012

Rossi, S., C. Gravili, G. Milisenda, M. Bosch-Belmar, D. De Vito, and S. Piraino. 2019. Effects of global warming on reproduction and potential dispersal of Mediterranean Cnidarians. Eur. Zool. J. **86**: 255–271. doi:10.1080/24750263.2019.1631893

Schlining, B. M., and N. Jacobsen Stout. 2006. MBARI's video annotation and reference system. Proceedings of the Marine Technology Society/Institute of Electrical and Electronics Engineers Oceans Conference. p. 1–5.

Schmidtko, S., L. Stramma, and M. Visbeck. 2017. Decline in global oceanic oxygen content during the past five decades. Nature **542**: 335–339. doi:10.1038/nature21399

Sherman, K. 1991. The large marine ecosystem concept: research and management strategy for living marine resources. Ecol. Appl. **1**: 349–360. doi:10.2307/1941896

Sillero, N. 2011. What does ecological modelling model? A proposed classification of ecological niche models based on their underlying methods. Ecol. Model. **222**: 1343–1346. doi:10.1016/j.ecolmodel.2011.01.018

St. John, M. A., A. Borja, G. Chust, M. Heath, I. Grigorov, P. Mariani, A. P. Martin, and R. S. Santos. 2016. A dark hole in our understanding of marine ecosystems and their services: Perspectives from the mesopelagic community. Front. Mar. Sci. **3**: 31. doi:10.3389/fmars.2016.00031

Stamatakis, A. 2014. RAxML version 8: A tool for phylogenetic analysis and post-analysis of large phylogenies. Bioinformatics **30**: 1312–1313. doi:10.1093/bioinformatics/btu033

Sutton, T. T., and others. 2017. A global biogeographic classification of the mesopelagic zone. Deep-Sea Res. I: Oceanogr. Res. Pap. **126**: 85–102. doi:10.1016/j.dsr.2017.05.006

Thuesen, E. V., and J. J. Childress. 1994. Oxygen consumption rates and metabolic enzyme activities of oceanic California medusae in relation to body size and habitat depth. Biol. Bull. **187**: 84–98. doi:10.2307/1542168

Thuesen, E. V., L. D. Rutherford, P. L. Brommer, K. Garrison, M. A. Gutowska, and T. Towanda. 2005. Intragel oxygen promotes hypoxia tolerance of scyphomedusae. J. Exp. Biol. **208**: 2475–2482. doi:10.1242/jeb.01655

Thurber, A. R., A. K. Sweetman, B. E. Narayanaswamy, D. O. B. Jones, J. Ingels, and R. L. Hansman. 2014. Ecosystem function and services provided by the deep sea. Biogeosciences **11**: 3941–3963. doi:10.5194/bg-11-3941-2014

Toyokawa, M., T. Toda, T. Kikuchi, and S. Nishida. 1998. Cnidarians and ctenophores observed from the manned submersible *Shinkai 2000* in the midwater of Sagami Bay, Pacific coast of Japan. Plankton Biol. Ecol. **45**: 61–74.

Venegas-Li, R., N. Levin, H. Possingham, and S. Kark. 2017. 3D spatial conservation prioritisation: Accounting for depth in marine environments. Methods Ecol. Evol. **9**: 773–784. doi:10.1111/2041-210X.12896

Vinogradov, G. M., and A. L. Vereshchaka. 2006. Zooplankton distribution above the Lost City (Atlantis massif) and broken spur hydrothermal fields in the North Atlantic according to the data of visual observations. Oceanology **46**: 217–227. doi:10.1134/S0001437006020081

Webb, T. J., E. vanden Berghe, and R. O'Dor. 2010. Biodiversity's big wet secret: The global distribution of marine biological records reveals chronic under-exploration of the deep pelagic ocean. PLoS One **5**: e10223. doi:10.1371/journal.pone.0010223

Youngbluth, M., T. Sørnes, A. Hosia, and L. Stemmann. 2008. Vertical distribution and relative abundance of gelatinous zooplankton, in situ observations near the Mid-Atlantic Ridge. Deep-Sea Research Part II: Topical Studies in Oceanography **55**: 119–125. doi:10.1016/j.dsr2.2007.10.002

Zweng, M. M., and others. 2018. World Ocean Atlas 2018, Volume 2: Salinity. A. Mishonov Technical Ed. NOAA Atlas NESDIS 82: 50.

Acknowledgments

We thank Virginia Moriwake (Hawaii University) for sharing Okeanos Explorer footage of *Solmissus* from the Northern Pacific and the Okeanos Explorer onboard teams for acquiring it. Sindre Gåsland (Subsea 7) and Tone Falkenhaug (Institute of Marine Research, Norway) are thanked for sharing ROV videography of a North Atlantic *Solmissus* specimen. Russell R. Hopcroft (University of Alaska Fairbanks) is thanked for *Solmissus* distribution data taken during the Gulf of Alaska R/V Sikuliaq cruise in 2019. Cathy Lucas (University of Southampton) is thanked for providing additional information regarding the *Solmissus* specimens published in Lucas and Reed (2009). We thank Brian Schlining (MBARI) for technical support with FathomNet and Dmitrii Panthiukhin (The Alfred Wegener Institute) for introducing the R package *ENMeval*. Philipp Neitzel is thanked for help with annotation and organizing the images of Cape Verdean *Solmissus*. Two anonymous reviewers are thanked for their constructive comments on the previous version of the manuscript. This publication was within the

scope of the Research Fellowship project VE 1192/1-1 to G.V., funded by the Deutsche Forschungsgemeinschaft (DFG). H.-J.H. acknowledges funding from the DFG via an Emmy Noether Research Junior Group awarded to H.-J.H. (HO 5569/2-1) and from GEOMAR's POF III and POF IV programs. This work was partially funded by Japan Society for the Promotion of Science (JSPS) KAKENHI grant number 20K06806 and NOAA Ocean Exploration grant NA22OAR0110189. We acknowledge support by the Open Access Publication Funds of Alfred-Wegener-Institut Helmholtz-Zentrum für Polar-und Meeresforschung. Open Access funding enabled and organized by Projekt DEAL.

Conflict of Interest

None declared.

Submitted 24 November 2022
Revised 26 June 2023
Accepted 06 July 2023

Associate editor: Kelly J. Benoit-Bird